Title
A STUDY OF THE BETA-DECAY ENERGIES OF HIGHLY NEUTRON-DEFICIENT INDIUM ISOTOPES

Author
Cerny, J.

Publication Date
1981-06-01

LBL-12853

Lawrence Berkeley Laboratory
UNIVERSITY OF CALIFORNIA

Presented at the Fourth International Conference on
Nuclei Far from Stability, Helsingor, Denmark,
June 7-13, 1981

A STUDY OF THE BETA-DECAY ENERGIES OF HIGHLY NEUTRON-DEFICIENT INDIUM ISOTOPES

Joseph Cerny, J. Äystö, M.D. Cable, P.E. Haustein,
R.F. Parry, H.M. Thierens, and J.M. Wouters

June 1981

NUCLEAR SCIENCE DIVISION

Prepared for the U.S. Department of Energy under Contract W-7405-ENG-48

LBL-12853

A STUDY OF THE BETA-DECAY ENERGIES OF HIGHLY NEUTRON-DEFICIENT INDIUM ISOTOPES

Joseph Cerny, J. Äystö, M. D. Cable, P. E. Haustein,
R. F. Parry, H. M. Thierens and J. M. Wouters

Department of Chemistry and Lawrence Berkeley Laboratory,
University of California, Berkeley, California 94720 (USA)

June 1981

This work was supported by the Director, U.S. Office of Energy Research, Division of Nuclear Physics of the Office of High Energy and Nuclear Physics, and by Nuclear Sciences of the Basic Energy Sciences Program of the U.S. Department of Energy under Contract No. W-7405-ENG-48.

A Study of the Beta-Decay Energies of Highly Neutron-Deficient Indium Isotopes[*]

Joseph Cerny, J. Äystö[†], M. D. Cable, P. E. Haustein[††], R. F. Parry, H. M. Thierens[†††] and J. M. Wouters.

Department of Chemistry and Lawrence Berkeley Laboratory, University of California, Berkeley, California 94720 (USA).

Abstract

Following on-line mass separations, the decay energies of $^{103-105}$In were measured by β-γ coincidence spectroscopy. The deduced masses of $^{103-105}$In are compared to the predictions of different available mass models. For ^{103}In an interesting deviation of -1 MeV from the trends of many theoretical systematic predictions is observed. A broad survey of the masses of the indium isotopes between the closed N=50 and N=82 shells is presented.

1. Introduction

The study of the nuclidic mass surface in the vicinity of the doubly magic nucleus ^{100}Sn is of fundamental interest in providing information on the strength of the shell closure when Z=N=50. A comparison of measured mass excesses with currently available model mass predictions can determine the accuracy with which the various models include the effects resulting from shell closures. Figure 1 presents a section of the chart of the nuclides in the vicinity of ^{100}Sn, depicting those nuclides with measured masses.

As a further step in the extension of the known mass surface, we report here the masses of $^{103-105}$In as calculated from our measured β-endpoint energies and the known decay schemes. The decay of ^{102}In was also observed, but with inadequate statistics up to now to determine an accurate endpoint energy. [The decay of this nucleus has only very recently been identified[1].] A comparison of the decay energies and deduced masses with different model

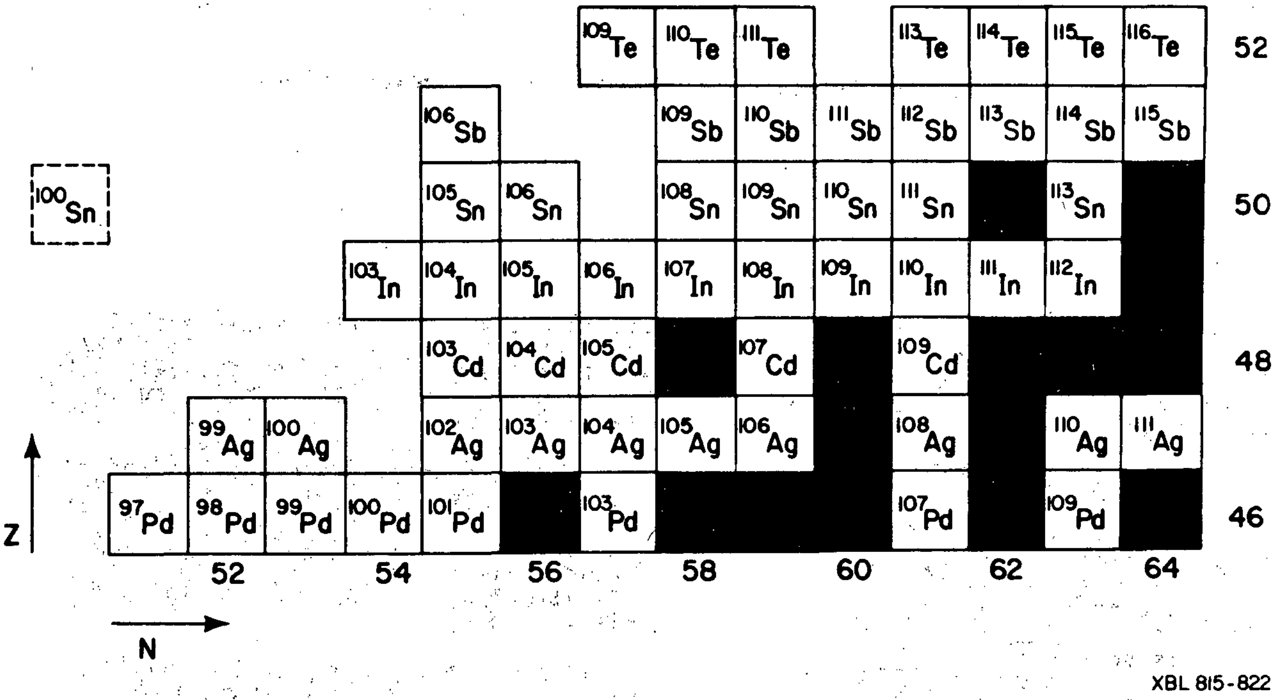

Fig. 1 A representation of the neutron-deficient nuclei with known masses for palladium through tellurium.

[†] Present address: University of Jyväskylä, Finland.
[††] Present address: Brookhaven National Laboratory, Upton, NY, USA.
[†††] On leave from the University of Gent, Belgium.
[*] This work was supported by the Director, U. S. Office of Energy Research, Division of Nuclear Physics of the Office of High Energy and Nuclear Physics, and by Nuclear Sciences of the Basic Energy Sciences Program of the U.S. Department of Energy under Contract No. W-7405-ENG-48.

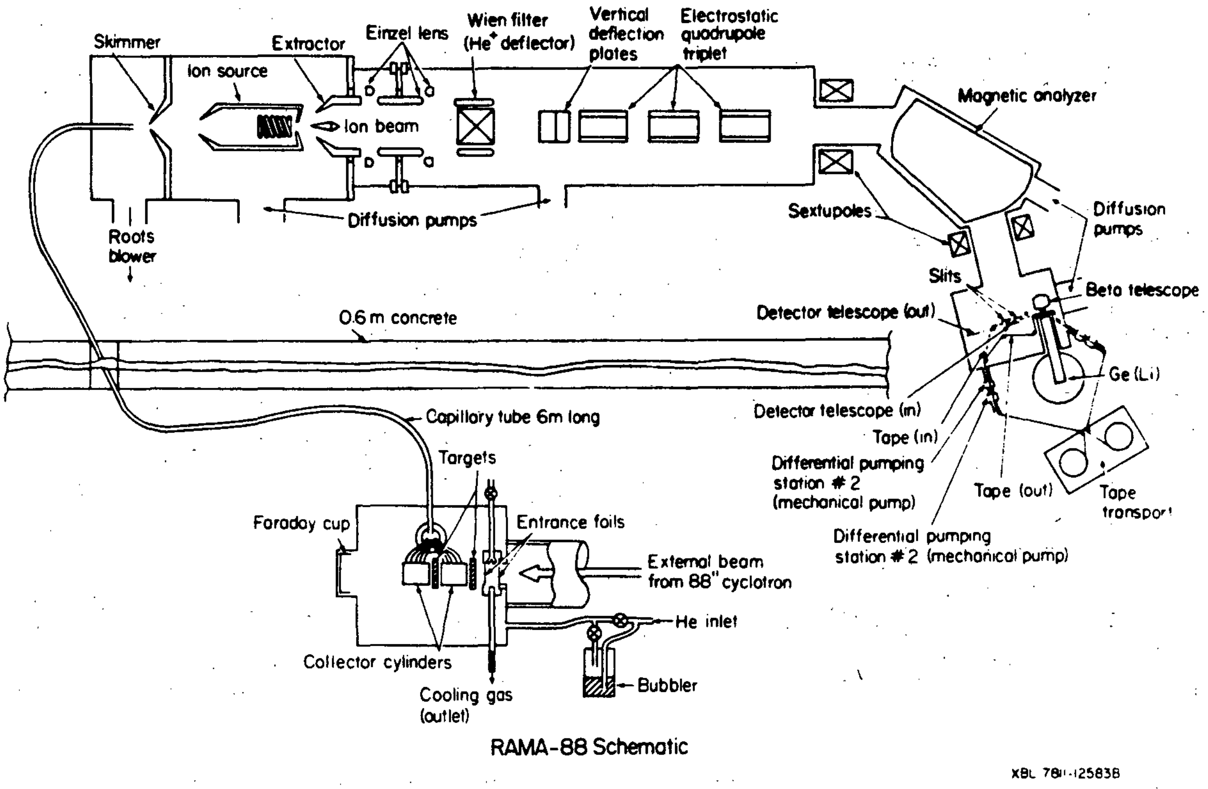

Fig. 2 Schematic view of the on-line mass separator RAMA.

predictions will be presented. In addition the systematics of the known ground state masses of the indium isotopes between the N=50 and 82 shells will be discussed.

2. Experimental

The indium isotopes of interest and various β-calibration sources were produced with the mass separator RAMA[2-4], located on-line at the Lawrence Berkeley Laboratory 88-inch cyclotron. This separator is novel in that reaction product recoils from the bombardment of multiple targets are thermalized in 1.5 atmospheres of helium and transported via a helium-jet to the hollow cathode ion source of the separator, operating at ∿1600°C (see fig. 2). After mass analysis, the separated activities were collected on mylar tape and rapidly transported to a detector station for β-γ coincidence spectroscopy. The β-telescope, positioned facing the radioactive source side of the tape, consisted of a 10 mm diameter and 1 mm thick NE102 plastic scintillator as a ΔE detector (for γ-ray rejection) and a large cylindrical NE102 plastic scintillator, 11.4 cm in both diameter and length, as an E detector. The γ-ray detector, located on the opposite side of the tape, was a large 15% Ge(Li) counter which was positioned within 1.0 cm of the β-ΔE detector to achieve high coincidence detection geometry. Standard fast-slow coincidence networks were set up between all three detectors with a final coincidence timing of 5 ns (FWHM) between the two scintillators and 20 ns (FWHM) between the β-E scintillator and the Ge(Li) counter.

Positron spectra obtained by gating these coincidence spectra with known transitions in the daughter nuclei were corrected for the finite energy resolution of the E detector using the procedure of Rogers and Gordon[5]. The response function of this detector was assumed to be that of a Gaussian curve, whose width varied with energy as $\sqrt{E}$[6]. This width was determined to be 200 keV using the 976 keV conversion electrons from ^{207}Bi. Energy endpoint determinations were obtained from weighted linear least-squares fits to Fermi-Kurie plots of the spectra. The Fermi-Kurie plot of the positron spectrum

Table I. Calibration Nuclei

Nuclide	Half-life	Gate (keV)	E^{max} (MeV)	Ref.	Reaction
^{38}K	7.6 min.	2168	2.724±0.002	7	^{24}Mg(^{16}O,pn)
^{62}Cu	9.7 min.	511	2.927±0.005	7	^{52}Cr(^{12}C,pn)
^{123}Cs	5.9 min.	98	3.410±0.122	7,22	^{nat}Cd(^{14}N,xn)
^{66}Ga	9.4 hr.	511	4.153±0.004	7	^{52}Cr(^{16}O,pn)
^{124}Cs	31 sec.	354	4.573±0.150	7,22	^{nat}Cd(^{14}N,xn)

of ^{62}Cu7) (one of the calibration nuclei) is presented in figure 3 as an example. An energy calibration as determined using the calibration activities listed in table I and the assumed response function was found to give a good linear fit. Table I also lists for each calibration activity the γ-gate employed to obtain the β spectrum and the reaction used for its production.

In order to study $^{103-105}$In, ^{14}N beams from 90 to 105 MeV and ^{16}O beams from 90 to 130 MeV were directed onto 80% enriched ^{92}Mo and natural Mo targets. All targets were 2 mg/cm^2 thick; the average beam intensity varied between 2 and 4 electrical μA.

3. Results

The Fermi-Kurie analysis of the positron spectrum from ^{105}In in coincidence with the 131 keV γ-transition in the ^{105}Cd daughter is shown in figure 4. About 27% of the decay is known to feed this 131 keV level directly, while the next strongly fed levels lie at 770 keV and 799 keV with branches of 8% and 9%, respectively (ref. 8). One can see the contribution of these higher levels from the change in slope of the Fermi-Kurie plot at ~3.0 MeV.

In the case of ^{104}In, 22% of the β-decay goes to the 4^+ level at 1492 keV, while the 2^+ level is not fed directly (ref. 9). This allows the use of both the 834 keV ($4^+ \rightarrow 2^+$ transition) and the 658 keV ($2^+ \rightarrow 0^+$ transition) as coincidence gates. Strong β-branches to levels at 2370, 2435 and 2492 keV are also present. This restricts the energy range for the least-squares fit to the data in the Fermi-Kurie plot to 1 MeV in the case of ^{104}In.

Figure 5 presents a Fermi-Kurie analysis for the ^{103}In positron spectrum in coincidence with the 188 keV transition in the ^{103}Cd daughter. Concerning the γ-decay of ^{103}In, a 720 keV γ-ray decaying with the proper half life was present in the γ-spectra in addition to the 188 keV and 202 keV γ-rays mentioned in ref. 10. The relative intensity of this γ-ray compared to the 188 keV γ-ray is 18±3%. Meyer et al.11) determined the level scheme of ^{103}Cd from the ^{94}Mo(^{12}C,3n) reaction. According to their work the 720 keV γ-ray depopulates the $11/2^+$ level at 908 keV and feeds the

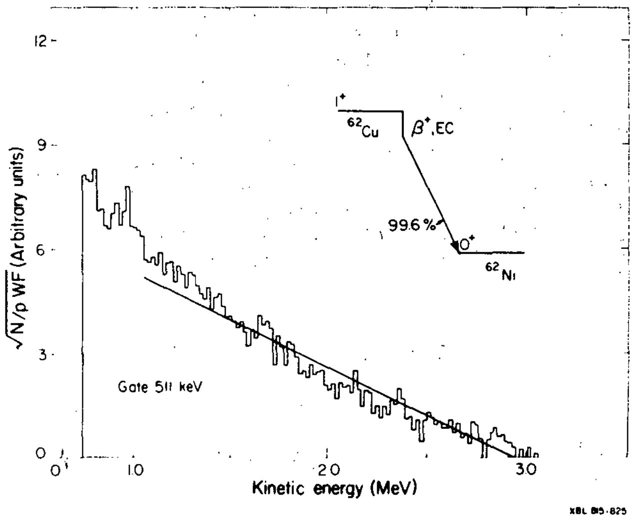

Fig. 3 Fermi-Kurie plot and partial decay scheme for ^{62}Cu. Ground state branching was taken from Ref. 7.

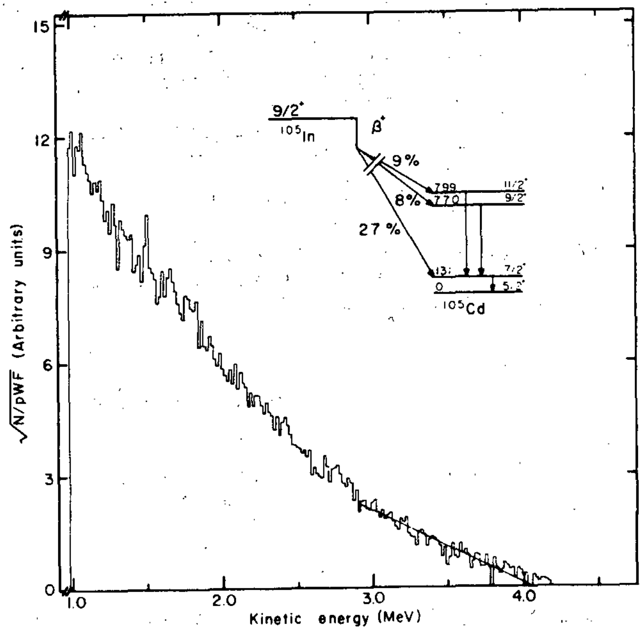

Fig. 4 Fermi-Kurie plot and partial decay scheme for ^{105}In. Beta-branching ratios were taken from Ref. 8.

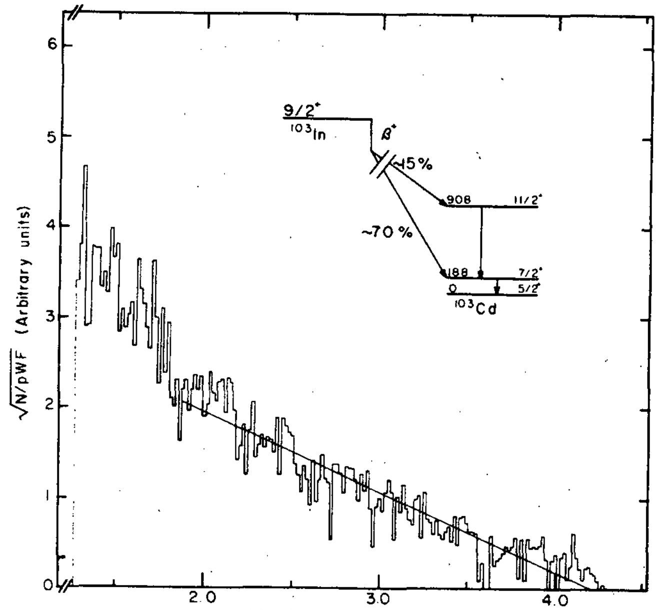

Fig. 5 Fermi-Kurie plot and partial decay scheme for ^{103}In. Beta-branching ratios were determined from Ref. 10 and our γ-spectrum.

$7/2^+$ level at 188 keV. Taking into account the relative intensities of the observed γ-rays, the β-branch to the level at 908 keV is about 5 times smaller than the branch to the first excited state at 188 keV. The linearity of the Fermi-Kurie plot is not affected seriously by the small β-feeding of the $11/2^+$ level as can be seen in figure 5.

A summary of our results on the $^{103-105}$In beta-decay energies is given in table II along with the coincident γ-rays used for the gating. For comparison the Q_{EC} values reported previously in the literature are also presented. The uncertainties quoted in our decay energies include the contribution from the energy calibration of the β-telescope. The decay energies for $^{103-104}$In obtained in this work agree quite well with the literature values and provide a significantly more precise Q_{EC} value for ^{103}In. A Q_{EC} value for ^{105}In was not previously available,

To investigate the β-decay of ^{102}In, β-γ coincidence measurements were carried out on mass 102 activities made in the reaction of 130 MeV ^{16}O on ^{92}Mo. In addition to known ^{102}Ag γ-rays, two equal intensity γ-rays at 777.2±0.5 keV and 862.1±0.5 keV were present in the γ-spectra. The half-life of these γ-rays was 21±7 sec according to our measurements. Very recently the decay of ^{102}In was also studied by Béraud et al.[1]. The results of their study, which will be presented in this conference, are in agreement with our observations. A preliminary experiment to measure the endpoint energy of ^{102}In has too low statistics to determine a decay energy with a reasonable precision. A further investigation is in progress.

4. Discussion

Information from the decay energy measurements of $^{103-105}$In can be used to delineate features of the mass surface in this region of nuclei. A comparison of the measured Q_{EC} values with the predictions of the available model masses can highlight which models are more successful in predicting the curvature of the mass surface. Converting the Q_{EC} values to mass excesses using the known cadmium masses also allows a direct comparison of the measured masses of $^{103-105}$In with the mass predictions.

Figure 6 shows the differences between the measured decay energies and the different model Q_{EC} predictions[12-14]. To deduce systematic trends this comparison extends to ^{108}In[15]. Each arrow in the figure is labeled by a number corresponding to the Q_{EC} prediction of a model as summarized in ref. 12; the Q_{EC} predictions of Möller and Nix[13] and of Monahan and Serduke[14] are also included. From figure 6 it is apparent that for $^{105-108}$In good agreement exists between the experimentally determined Q_{EC} values and the calculated values of the shell model formula of Liran and Zeldes[12d] and the mass formulas based on the relationships of the Garvey-Kelson type: Jänecke[12e], Comay and Kelson[12f], Jänecke and Eynon[12g] and Monahan and Serduke[14]. By ^{103}In, however, the Q_{EC} predictions of these mass formulas are systematically 1 MeV too high. The deviations between the Q_{EC} values, calculated with the droplet models of Myers[12a], Groote et al.[12b] Seeger

Table II. Summary of the Q_{EC} Determinations

Nuclide	Gate (keV)	Level in daughter (keV)	Q_{EC} (MeV) This Work	Q_{EC} (MeV) Literature
^{103}In	188	188	5.41±0.19	5.8±0.5 (ref. 10)
^{104}In	658,834	658,1492	7.41±0.20	7.1±0.2 (ref. 9)
^{105}In	131	131	5.16±0.16	----

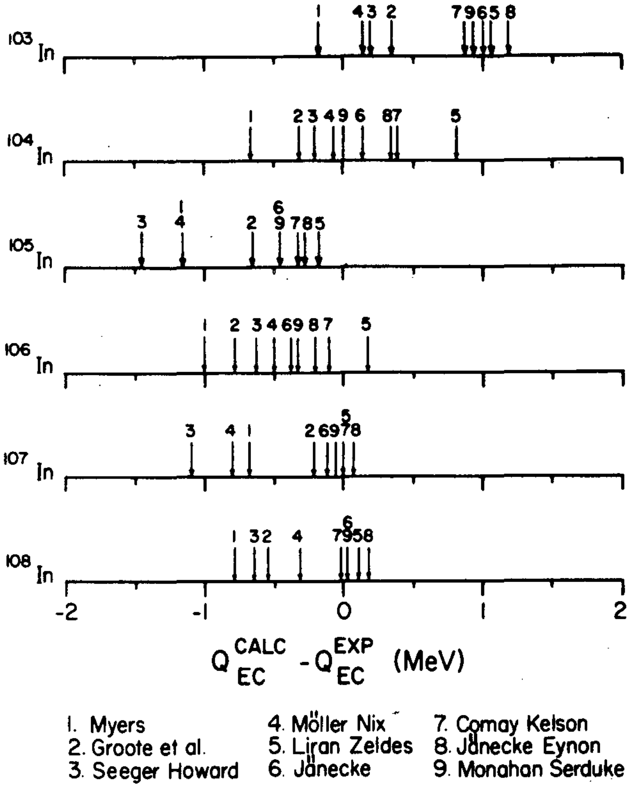

XBL 815-819

Fig. 6 Comparison of experimentally determined Q_{EC} values with the predictions of selected model mass formulas.

and Howard [12c] and Möller and Nix[13]), and the experimental values are larger than for the other mass formulas. In addition, until ^{103}In, these droplet model predictions are systematically too low.

Table III shows the mass-excess values for $^{103-105}$In, determined from the measured Q_{EC} values, using the experimentally known masses of the cadmium isotopes (ref. 15-17). The differences between the measured masses and the available mass predictions are also given in table III. The mass of ^{105}In is predicted adequately by the Liran-Zeldes[12d]), Comay-Kelson[12f]) and Janecke-Eynon[12g]) mass formulas, taking into account the error in the calculated mass of ^{105}In, quoted in ref. 12f: 350 keV. For the mass of ^{103}In the predictions of the Liran-Zeldes and Garvey-Kelson type mass formulas are systematically about 1 MeV too high, as already noted for the Q_{EC} values.

By also considering the available data on the neutron-rich indium isotopes, one can observe the broad systematics of their ground state mass behavior as a function of the neutron number between the shell closures at N=50 and N=82. Aleklett et al.[18]) studied the masses of ^{120}In-^{129}In. The mass of the N=82 nucleus ^{131}In can be deduced from the recently reported Q_{EC} values of ^{131}In (ref. 19) and ^{131}Sn (ref. 20) and the experimentally-determined mass of ^{131}Sb (ref. 21)

Figures 7 and 8 show comparisons of the predictions of the known indium masses with selected representatives of the different mass theories which are available. Those masses calculated according to the mass relations of the Garvey-Kelson type and those calculated from the shell model formula of Liran-Zeldes agree very well with the experimental results from ^{106}In to ^{125}In (fig. 7). For each of these mass models the root-mean-square deviation of theory from experiment for these nuclides is less than 200 keV. For the more neutron-rich In isotopes, approaching the closed N=82 shell, these mass predictions diverge and the deviations from the experimental values increase; an exception is the predictions of Comay and Kelson, which reproduce fairly well the experimental masses. On the neutron-deficient side of figure 7, at ^{103}In, a strong deviation of about 1 MeV of the experimental value from the predictions of Liran-Zeldes and the different Garvey-Kelson type mass formulas suddenly appears. The model of Comay-Kelson (ensemble averaging of mass values using the Garvey-Kelson transverse relation) exhibits the best predictive qualities for the indium isotopes over the A=103 to 131 mass range: the root-mean-square deviation from the experimental data is only 240 keV. In the case of the Liran-Zeldes, Jänecke, Jänecke-Eynon and Monahan and Serduke models, root-mean-square values of 330, 320, 640 and 340 keV, respectively, are obtained.

Table III. Summary of Experimental Mass Excesses and Comparison with Different Model Mass Predictions.

Nuclide	Mass excess (MeV)	$M_{exp} - M_{calc}$ (MeV)								
		a	b	c	d	e	f	g	h	i
^{103}In	-75.21±0.19	0.70	-0.99	0.59	-0.70	-1.17	-0.78	-0.78	-1.10	-0.72
^{104}In	-76.31±0.20	1.00	-0.50	1.29	-0.11	-0.58	0.18	-0.07	-0.19	0.26
^{105}In	-79.18±0.16	1.25	-0.06	1.92	0.48	0.28	0.59	0.40	0.28	0.58

a) Myers; b) Groote et al.; c) Seeger-Howard; d) Möller-Nix; e) Liran-Zeldes; f) Jänecke; g) Comay-Kelson; h) Jänecke-Eynon; i) Monahan-Serduke.

The predictions of those liquid drop models considered here differ more from the experimentally observed mass behavior than the results of calculations based on the Garvey-Kelson relations (see figure 8). For the models of Myers, Groote et al., Seeger-Howard and Möller-Nix the root-mean-square deviation from all the indium mass data is 1070, 830, 780 and 630 keV, respectively. As was noted for those mass models displayed in figure 7, a sudden change in the systematic differences between the experimental and calculated masses also sets in for ^{103}In in the comparison with the liquid drop model predictions shown in figure 8.

In conclusion, according to our results, ^{103}In is about 1 MeV more bound than predicted by the Liran-Zeldes and the different Garvey-Kelson type mass formulas, which reproduce very well the heavier indium mass data. A similar effect is not present for the neutron-rich indium isotopes in the vicinity of the N=82 closed shell. An extension of this study to the lighter indium isotopes and other investigations of the mass surface near ^{100}Sn will show whether the observed deviation from the systematics for ^{103}In might have any possible relationship with the nearby double-shell closure.

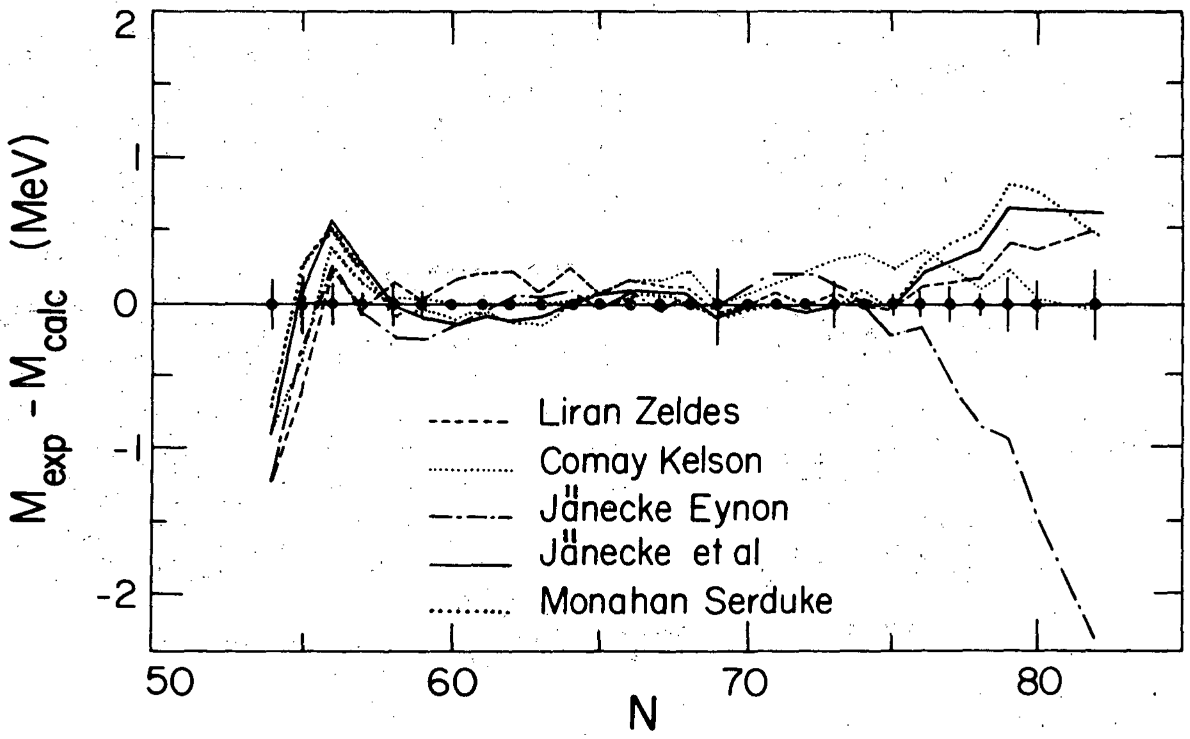

XBL 815-823

Fig. 7 A comparison of known indium masses with the predictions of the Liran-Zeldes and the Garvey-Kelson type mass equations.

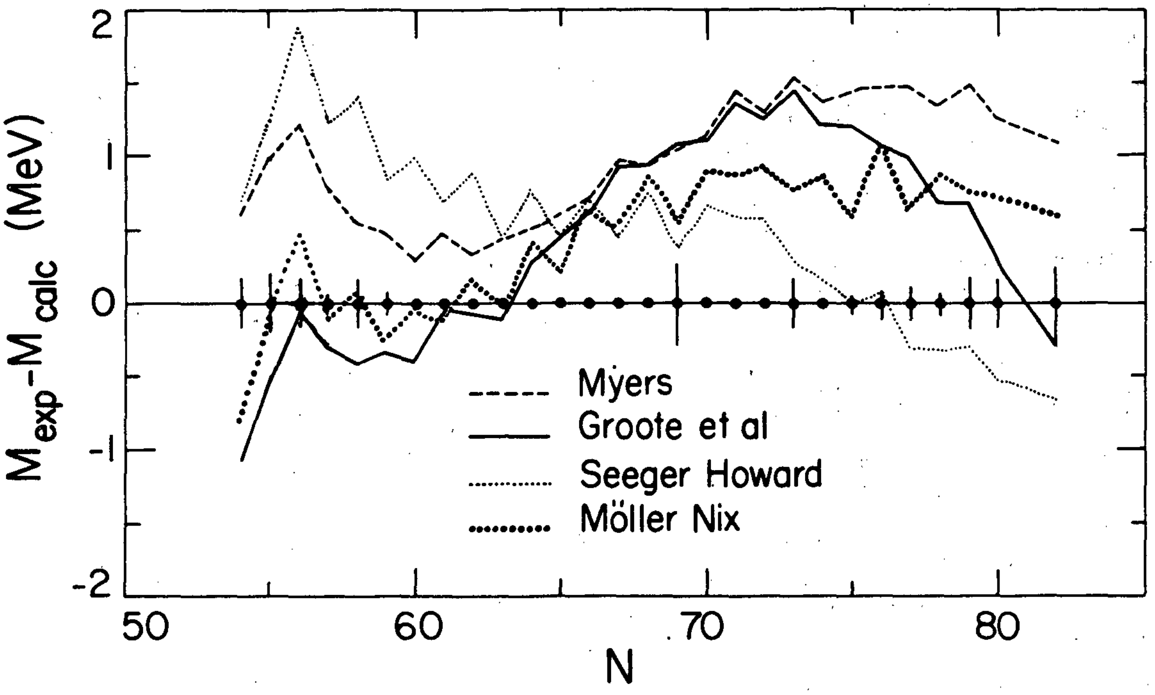

XBL 815-824

Fig. 8 A comparison of known indium masses with the predictions of different liquid drop model mass equations.

References

1. R. Béraud, J. Tréherne, A. Charvet, R. Duffait, J. Genevey, A. Gizon, J. Gizon, and M. Meyer, Z. Physik A299 (1981) 279.

2. D. M. Moltz, R. A. Gough, M. S. Zisman, D. J. Vieira, H. C. Evans and J. Cerny, Nucl. Instr. Meth. 172 (1980) 507.

3. D. M. Moltz, J. M. Wouters, J. Äystö, M. D. Cable, R. F. Parry, R. D. von Dincklage and J. Cerny, Nucl. Instr. Meth. 172 (1980) 519.

4. D. M. Moltz, J. Äystö, M. D. Cable, R. F. Parry, P. E. Haustein, J. M. Wouters and J. Cerny, presented at the Electromagnetic Isotope Separator-10 Conference, Zinal, Switzerland, September 1-6, 1980.

5. P. C. Rogers and G. E. Gordon, Nucl. Instr. Meth. 37 (1965) 259.

6. E. Beck, Nucl. Instr. Meth. 76 (1969) 77.

7. C. M. Lederer and V. S. Shirley, editors, Table of Isotopes, 7th edition, John Wiley and Sons, New York, 1978.

8. I. N. Wischnewski, H. V. Klapdor, P. Herges, H. Fromm and W. A. Zheldonozhski, Z. Physik A298 (1980) 21.

9. H. Huang, B. P. Pathak and J. K. P. Lee, Can. J. Phys. 56 (1978) 936.

10. G. Lhersonneau, G. Dumont, K. Cornelis, M. Huyse and J. Verplancke, Phys. Rev. C 18 (1978) 2688.

11. M. Meyer, R. Béraud, A. Charvet, R. Duffait, J. Tréherne and J. Genevey, Phys. Rev. C 22 (1980) 589.

12 a) W. D. Myers, At. Data Nucl. Data Tables 17 (1976) 411.

b) H. V. Groote, E. R. Hilf and K. Takahashi, ibid. 418.

c) P. A. Seeger and W. M. Howard, ibid. 428.

d) S. Liran and N. Zeldes, ibid. 431.

e) J. Jänecke, ibid. 455.

f) E. Comay and I. Kelson, ibid. 463.

g) J. Jänecke and B. P. Eynon, ibid. 467.

13. P. Möller and J. Nix, Report LA-UR-80-1996.

14. J. E. Monahan and F. J. D. Serduke, Phys. Rev. C 17 (1978) 1196.

15. A. H. Wapstra and K. Bos, At. Data Nucl. Data Tables 19 (1977) 177.

16. R. C. Pardo, E. Kashy, W. Benenson and L. W. Robinson, Phys. Rev. C 18 (1978) 1249.

17. A. Plochocki, G. M. Gowdy, R. Kirchner, O. Klepper, W. Reisdorf, E. Roeckl, P. Tidemand-Petersson, J. Zylicz, U. J. Schrewe, R. Kantus, R. D. von Dincklage and W. D. Schmidt-Ott, Nucl. Phys. A332 (1979) 29.

18. K. Aleklett, E. Lund and G. Rudstam, Phys. Rev. C 18 (1978) 462.

19. L. E. De Geer and G. B. Holm, Phys. Rev. C 22 (1980) 2163.

20. U. Keyser, H. Berg, F. Munnich, K. Hawerkamp , H. Schrader, B. Pfeiffer and E. Monnand, Z. Physik A289 (1979) 407.

21. E. Lund, K. Aleklett and G. Rudstam, Nucl. Phys. A286 (1977) 403.

22. M. Epherre, G. Audi, C. Thibault, R. Klapisch, G. Huber, F. Touchard and H. Wollnik, Phys. Rev. C 19 (1979) 1504.

TECHNICAL INFORMATION DEPARTMENT
LAWRENCE BERKELEY LABORATORY
UNIVERSITY OF CALIFORNIA
BERKELEY, CALIFORNIA 94720